Tropical stratospheric aerosol layer from CALIPSO lidar observations

Jean-Paul Vernier, Jean-Pierre Pommereau, Anne Garnier, Jacques Pelon, Niels Larsen, Johannes K. Nielsen, Tina Christensen, Francesco Cairo, Larry W. Thomason, Thierry Leblanc, et al.

Tropical stratospheric aerosol layer from CALIPSO lidar observations

J. P. Vernier,[1] J. P. Pommereau,[1] A. Garnier,[1] J. Pelon,[1] N. Larsen,[2] J. Nielsen,[2] T. Christensen,[2] F. Cairo,[3] L. W. Thomason,[4] T. Leblanc,[5] and I. S. McDermid[5]

Received 20 February 2009; revised 4 August 2009; accepted 31 August 2009; published 22 December 2009.

[1] The evolution of the aerosols in the tropical stratosphere since the beginning of the Cloud-Aerosol Lidar and Infrared Pathfinder Satellite Observation (CALIPSO) mission in June 2006 is investigated using Cloud-Aerosol Lidar with Orthogonal Polarization (CALIOP) lidar data. It is shown that the current operational calibration requires adjustment in the tropics. Indeed, on the basis of the assumption of pure Rayleigh scattering between 30 and 34 km the current calibration leads to an average underestimation of the scattering ratio by 6% because of the significant amount of aerosols up to 35 km altitude in the tropics, in contrast to midlatitudes. A better result is obtained by adjusting the calibration to higher altitudes, 36–39 km, where past Stratospheric Aerosol and Gas Experiment (SAGE) II extinction measurements showed an almost complete absence of aerosols. After recalibration the tropical stratospheric aerosol picture provided by CALIOP during the first 2 years of the mission reveals significant changes in the aerosol concentration associated with different transport processes. In the stratosphere the slow ascent of several volcanic layers and their meridional transport toward the subtropics are very consistent with the Brewer-Dobson circulation. The near-zero vertical velocity observed around 20 km during the Northern Hemisphere (NH) summer is in good agreement with radiative heating calculation. In the Tropical Tropopause Layer (TTL), weak depolarizing particles are observed during land convective periods, particularly intense over South Asia during the monsoon season. Finally, seasonal fast occurrence of apparent clean air in the TTL during the NH winter requires more investigations to understand its origin.

Citation: Vernier, J. P., et al. (2009), Tropical stratospheric aerosol layer from CALIPSO lidar observations, *J. Geophys. Res.*, *114*, D00H10, doi:10.1029/2009JD011946.

1. Introduction

[2] All chemical species and greenhouse gases controlling stratospheric ozone chemistry and climate have their sources at the surface and are lofted into the upper troposphere by tropical convection. They are then transported more or less rapidly across the Tropical Tropopause Layer (TTL) into the lower stratosphere before being distributed on a global scale in the stratosphere by the Brewer-Dobson circulation [*Brewer*, 1949; *Holton et al.*, 1995]. Though this scheme is generally accepted, the contribution to the vertical transport from the Level of Neutral Buoyancy (LNB) around 14 km to the top of the TTL at around 19 km by convective overshooting [*Danielsen*, 1982, 1993; *Sherwood and Dessler*, 2000; *Pommereau and Held*, 2007] compared to slow ascent by diabatic radiative heating [*Hartmann et al.*, 2001; *Holton and Gettelman*, 2001; *Corti et al.*, 2005; *Fu et al.*, 2007; *Yang et al.*, 2008] is still debated. The sporadic occurrence of deep overshoots is generally accepted but their impact on a global scale is still questionable [*Fueglistaler et al.*, 2009] since they are thought to rarely occur and thus be of limited global-scale importance. However, recent satellite observations of tropospheric species such as N_2O, CH_4 and CO in the tropical Upper Troposphere and Lower Stratosphere (UTLS) [*Ricaud et al.*, 2007; *Liu*, 2007; *Liu et al.*, 2007; *Ricaud et al.*, 2009], showing high correlation between the largest concentrations of these species and overshooting precipitation features reported by the TRMM satellite Precipitation Radar [*Liu and Zipser*, 2005], would suggest that deep convection over land could have a significant impact on the tropical UTLS. The objective of the present study is to investigate the vertical transport in the tropical UTLS from the aerosols measured by the Cloud-Aerosol Lidar with Orthogonal Polarization (CALIOP) lidar onboard Cloud-Aerosol Lidar and Infrared Pathfinder Satellite Observation (CALIPSO) [*Winker et al.*, 2003, 2007] which, as shown by the Lidar in Space Technology Experiment (LITE) 10 day precursor mission [*Osborn et al.*, 1998] and the Stratospheric Aerosol and Gas Experiment (SAGE) II observations [*Chu et al.*, 1989; *McCormick and Veiga*, 1992; *Trepte and Hitchman*, 1992; *McCormick et al.*, 1995] are excellent tracers of stratospheric circulation. The advantage of CALIOP for this is the better vertical resolution and sampling in the tropics compared to

[1]LATMOS, Université de Versailles Saint Quentin, CNRS, Verrières le Buisson, France.
[2]Danish Meteorological Institute, Copenhagen, Denmark.
[3]ISAC-CNR, Rome, Italy.
[4]NASA Langley Research Center, Hampton, Virginia, USA.
[5]Jet Propulsion Laboratory, California Institute of Technology, Wrightwood, California, USA.

0148-0227/09/2009JD011946

SAGE II [*Hitchman et al.*, 1994]. The potential of CALIOP for detecting small volcanic plumes in the lower tropical stratosphere was already demonstrated by *Thomason et al.* [2007] but problems with the current calibration of the instrument were also suggested. Here, a method for adjusting the calibration and optimum space and time averages is proposed with which a better description of the time evolution of the aerosols since the launch of CALIPSO was derived.

[3] Section 2 provides a description of the processing applied to current operational products, leading to a first picture of the evolution of stratospheric aerosols from June 2006 to September 2008. An improved calibration procedure, together with an appropriate cloud mask, are proposed in section 3 and further validated by comparisons with past SAGE II observations, and contemporary in situ balloon and ground-based lidar observations. The revised picture of the time evolution of the aerosols above 15 km since the beginning of the mission and altitude-latitude cross sections at selected periods are shown in section 4, followed by a discussion of the implications for the vertical transport in the lower stratosphere and conclusions in section 5.

2. Stratospheric Aerosols Picture From Current CALIOP Operational Products

[4] Because of their better signal to noise compared to the daytime and the 1064 nm data, only CALIOP lidar nighttime measurements at 532 nm are used. The data utilized are the Total Attenuated Backscatter coefficients, β'_{532} available from the CALIOP level 1B V2.01 analysis. Also, the measurements in the South Atlantic magnetic Anomaly (SAA) are discarded because of their larger noise. After applying adequate temporal and horizontal averaging to increase the S/N ratio, a correction for the two-way transmission is applied.

2.1. Three-Dimensional Regular Grid

[5] The CALIOP level 1B product consists of about 15 half-orbits per night, with measurements at 333 m horizontal resolution (about 300 profiles per degree latitude) and vertical resolution of 60 m, 180 m, and 300 m within in the altitude ranges 8.2–20.2 km, 20.2–30.1 km, and 30.1–40.0 km, respectively. The Earth is fully covered in 16 days or 233 orbits separated by about 1.54 degrees longitude [*Winker et al.*, 2003]. The whole CALIOP data set has been arranged in a series of 16 day time resolution 3-D grids of 1° latitude × 2° longitude × 200 m height. Each grid is fully completed every 16 days, each cell containing level 1B parameters averaged over 300 to 600 profiles. The data between 95°W and 15°E longitude and 50°S and 10°N latitude are discarded to avoid the SAA.

2.2. Molecular Attenuation, Ozone Absorption, and Scattering Ratio

[6] The total attenuated backscatter coefficient profiles are corrected for molecular attenuation and ozone absorption [*Vaughan et al.*, 2004] in each cell of the grid defined in 2.1. The attenuation by aerosols is neglected because of the small optical depth of less than 0.002 during this non volcanic period [*Thomason and Peter*, 2006]; corresponding to a transmission greater than 0.995 at 15 km.

[7] The scattering ratio (SR) is then calculated, defined as the ratio of β'_{532} previously corrected and the molecular backscatter coefficient (β_m) calculated from air density provided by the GEOS 5 global model of the NASA Global Modeling and Assimilation Office (GMAO), and the Rayleigh scattering cross section given in the CALIOP Algorithm Theoretical Basis Document [*Hostetler et al.*, 2006].

2.3. Data Averaging

[8] The standard deviation of the mean scattering ratio resulting from the averaging of 300 measurements in a cell is on the order of ±140%. Therefore, an unambiguous identification of aerosol layers requires more averaging. The full zonal means between 20°S and 20°N, obtained by averaging 7200 cells leading to a precision of about ±1.6%, are used in the following discussion.

2.4. Time Evolution of Stratospheric Aerosols in the Tropical Belt Since June 2006

[9] Figure 1 displays the altitude-time cross section of the SR zonal mean between 20°S and 20°N from July 2006 to September 2008 with a 16 day time resolution. The SR varies from 0.94, a value smaller than pure Rayleigh scattering, to 1.20 at 20 km at the beginning of the CALIOP observations in June 2006 and to even larger values below 18 km where clouds are frequent. The cloud top height varies between 16.5 km in August–September and 18 km from December to February. This is above the zonal mean tropopause height indicated by the 370 K level which varies between 15.8 km in the summer and 16.2 km in the winter. The dense aerosol plume around 20 km, already present at the beginning of the mission in June 2006, is attributed to the eruption of the Soufrière Hills volcano in Monserrat Island in the Caribbean on 20 May 2006, whose SO_2 cloud was observed during the week after the eruption by the AURA-OMI satellite [*Carn et al.*, 2007; *Prata et al.*, 2007] (http://so2.umbc.edu/omi/omi_images.html). The plume was also observed by all balloon in situ instruments flown in Niamey at 13°N in Niger in August 2006 during a SCOUT-AMMA campaign dedicated to the study of convective overshooting [e.g., *Khaykin et al.*, 2009]. The measurements showed that the particles were made of 0.1 μm mean radius spherical droplets (T. Deshler, personal communication, 2008), consistent with their sulfate aerosol nature. The further slow rise of the plume, at an average vertical velocity of 0.2–0.3 km/month after November 2006 and displaying a tape recorder–like feature similar to that of water vapor [*Mote et al.*, 1996], is very consistent with the upwelling velocity of the Brewer-Dobson circulation. Though partially masked by clouds, another volcanic plume can be seen around 18 km in November 2006 after the eruption of Tavurvur in Papua New Guinea on 7 October 2006, but disappears rapidly in December–January.

[10] However, the picture also shows inconsistent features. SR values lower than unity are observed in the upper stratosphere above 34 km as well as in the lower stratosphere between the cloud tops and 20 km in both years during the March–May period. This suggests some aerosol cleansing although the SR values are unrealistically low. The sudden simultaneous SR changes at all levels up to 40 km (i.e., the sudden rise in May–June 2007 or the drop in the next year in January–April 2008) are not consistent with any known atmospheric process. Since the 30–34 km range has been selected as an aerosol free reference point for the operational

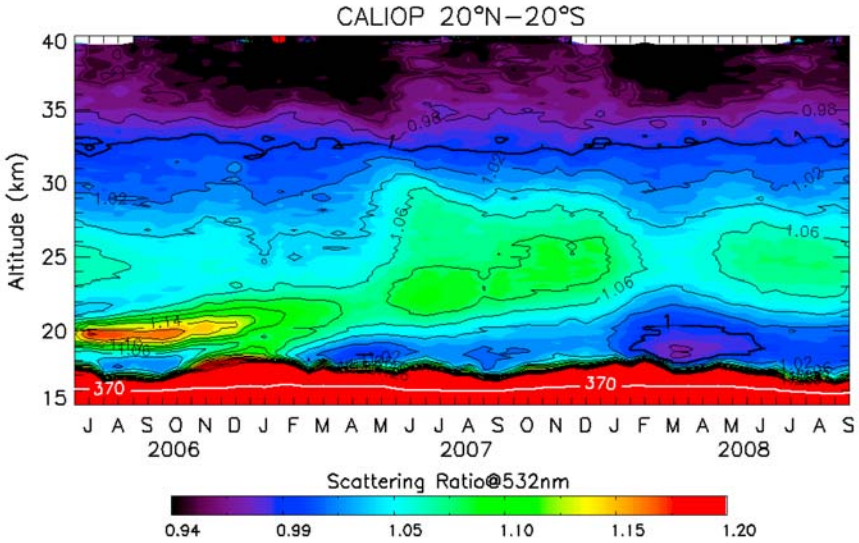

Figure 1. Time evolution of the zonal mean [20°S−20°N] CALIOP SR standard product profiles from July 2006 to September 2008 (SR = 1 isoline bold). The maximum cloud top height (SR > 1.24 in red) varies between 17 and 18 km. Also shown is the 370 K level indicative of the tropopause height.

processing, as a trade-off between low aerosol loading and acceptable signal-to-noise ratio [*Hostetler et al.*, 2006], the CALIOP SR is constant and equal to one at this level. However, this assumption is not valid in the tropics where the SAGE II measurements in 2001−2005 showing significant aerosol extinction at these altitudes. Indeed, after conversion into SR, using a backscatter-to-extinction ratio of 0.02 sr^{-1} representative of the Northern Hemisphere stratospheric background aerosols [*Jäger et al.*, 1995; *Jäger and Deshler*, 2002], it shows an underestimation of the mean tropical SR by 2 to 12%. Since the 36−39 km altitude range is almost aerosol free with SR of 1.02 ± 0.03 according to SAGE II, this range will be used in the following as the new reference to adjust the calibration.

3. Improved Calibration, Cloud Mask, and Validation

[11] This section describes the adjustment of the CALIOP calibration and the cloud mask applied to extend the aerosol retrieval below the cloud top level, and the validation of the results by comparison with in situ balloon and ground-based lidar measurements available in the tropics from 2006 to 2008.

3.1. Calibration Adjustment

[12] The calibration is adjusted following the same approach as the operational processing but using the 36−39 km altitude range as the aerosol free reference instead of 30−34 km. An adjusted scattering ratio profile SR_{ad} is calculated by averaging the SR profiles within 4° longitude × 1° latitude boxes using the following the formula.

$$SR_{ad}[i,j,k] = SR[i,j,k] x C_{ad}[i,j] \quad (1)$$

$$\text{where } C_{ad}[i,j] = {}^{1}\Big/_{\overline{SR}_{36-39\,km}[i,j]} \quad (2)$$

is the normalization factor in each 4° longitude × 1° latitude box, further smoothed over 12 boxes within 36° longitude × 3° latitude. The i, j, and k indices refer to the latitude, longitude, and altitude bins, respectively.

[13] Figure 2 shows the latitude-time variation of C_{ad} derived by this procedure which is also representative of the aerosol SR (SR_{ad}) between 30 and 34 km. It shows little adjustment with $C_{ad} \leq 1.02$ at midlatitude indicating that the current CALIOP calibration at 30−34 km is adequate there. In contrast, large amplitude temporal modulations between 2 and 12% are observed in the tropics. Shown on the right in Figure 3, is the latitude-time CALIOP SR_{ad} variation at 30−34 km, and on the left, the SAGE II aerosol extinction at 1020 nm at the same altitude from 2001 to 2005, together with the Singapore zonal wind at 10 hPa. The aerosol loading is higher during the westerly phase of the QBO and sudden changes of concentration are highly correlated with changes from westerly to easterly winds. The similarities between CALIOP SR_{ad} and SAGE II extinction confirms that these variations are real, resulting from the springtime increase of meridional exchange alternately in both hemispheres reinforced by the apparent lofting of the aerosols during the east phase of the QBO [*Trepte and Hitchman*, 1992]. The larger noise in the Southern Hemisphere the CALIPSO results is due to the reduced number of profiles after the removal of 30% of the data in the SAA area.

3.2. Cloud Mask

[14] Cirrus clouds and cumulo-nimbus anvils up to 18 km are frequent in the tropical belt and their occurrence has been studied using SAGE II, CloudSat and CALIPSO data [*Wang et al.*, 1996; *Liu*, 2007; *Sassen et al.*, 2008; *Nazaryan et al.*, 2008]. Since these clouds are made of ice crystals they are depolarizing and thus can be separated from nondepolarizing aerosol liquid droplets. A cloud mask has been derived from the depolarization ratio, defined as the ratio of perpendicular to total backscatter at 532 nm [*Cairo et al.*, 1999] for each cell of the 3D 2° longitude × 1°latitude × 200 m height grid,

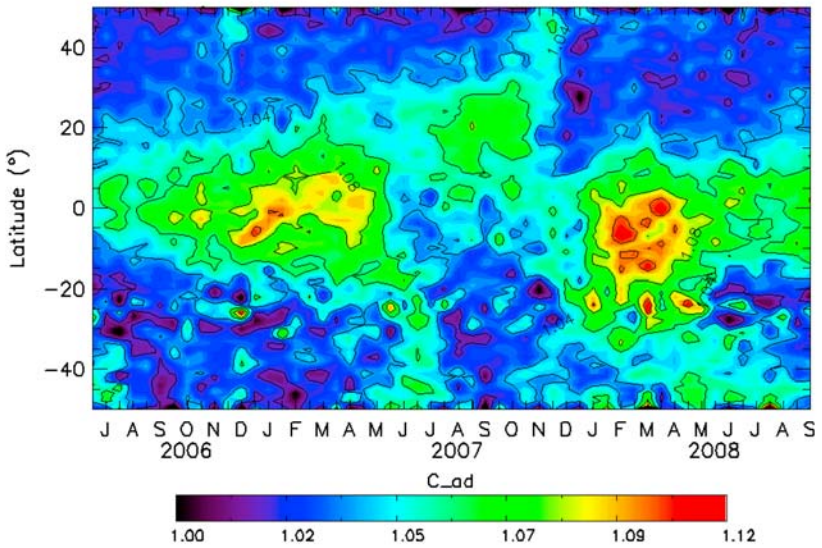

Figure 2. Latitude-time cross section of the calibration coefficient (C_{ad}) adjusted assuming the 36–39 km level is aerosol-free (SR_{ad} = 1). The picture is thus representing the revised aerosol scattering ratio (SR_{ad}) between 30 and 34 km.

which removes all the data below the altitude where a given threshold is encountered. Figure 4 shows the cloud occurrence between 15 and 20 km with a 16 day time resolution defined as the percentage of cloudy cells detected when applying a 5% depolarization ratio threshold. It decreases from an average 60% at 15 km to 1–3% at 20 km, with a broad maximum during the Northern Hemisphere winter and spring. The apparent cloud occurrence increase over the 2 years above 17 km seems to be an artifact due to increasing noise in the depolarization ratio as shown by the increase of the standard deviation from 0.5% to 0.7% (not shown). However, the seasonal maximum displays a double peak feature, the first in December–January and the second though of lesser amplitude in April–May. The seasonal variation is highly consistent with the SAGE II picture of subvisual cloud occurrence frequency at 17.5 km [*Wang et al.*, 1996] and the global distribution of cirrus clouds identified from CloudSat-Calipso [*Sassen et al.*, 2008]. As displayed by these pictures and further analyzed by *Liu* [2007], the December–January peak results from the dominant high 60–70% cirrus occurrence frequency over the west Pacific during the season of highest and coldest tropopause. In contrast, as shown by *Liu and Zipser* [2005], the April–May peak is strongly weighted by a maximum cloud frequency at

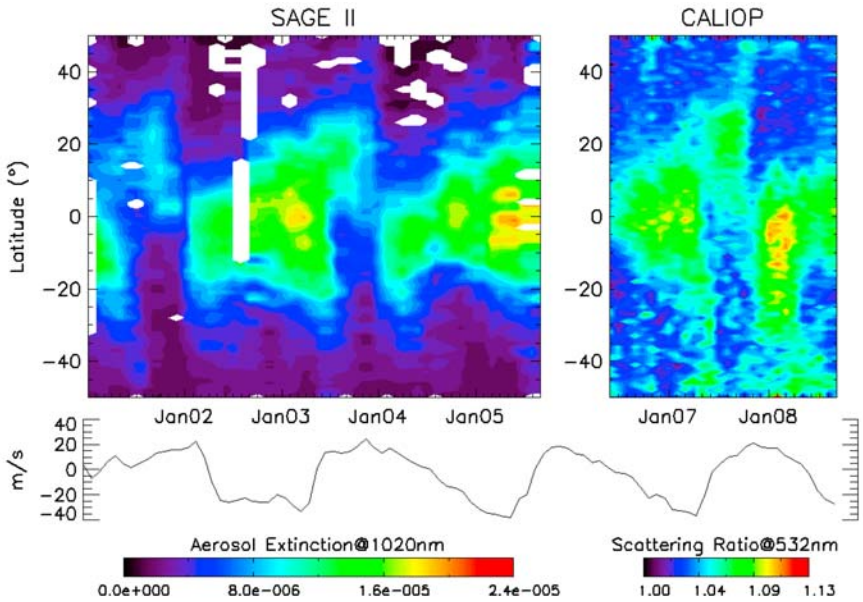

Figure 3. (left) Latitude-time cross section of SAGE II aerosol extinction at 1020 nm at 30–34 km in 2001–2005 and (right) CALIOP SR at the same altitude after recalibration. (bottom) QBO phase from Singapore zonal wind at 10 hPa.

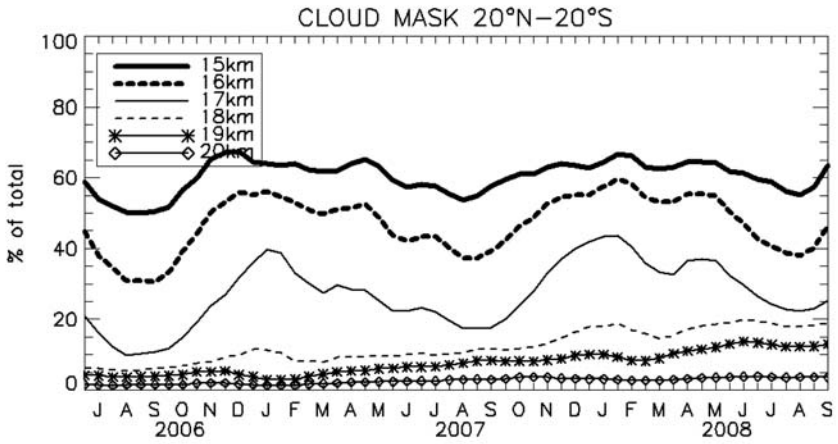

Figure 4. Frequency of occurrence of cloud removal by the cloud mask.

16–18 km over Africa and to a smaller extent South America, displaying in addition higher frequencies at night compared to day, absent over oceanic regions, thus suggesting anvils related to convective systems developing in the afternoon over land [*Sassen et al.*, 2008; *Liu and Zipser*, 2009].

3.3. Comparison With in Situ Balloon Measurements

[15] The corrected CALIOP SR profiles have been compared to backscatter-sonde (BKS) [*Rosen and Kjome*, 1991] and balloon-borne diode laser (LABS) [*Adriani et al.*, 1996] measurements carried out during two SCOUT-AMMA campaigns dedicated to the study of convection in Niamey (13°N, 2°E) in Niger in August 2006 [*Cairo et al.*, 2009] and September 2008. The mean SR profiles shown are averages from 9 BKS and 4 LABS flights in 2006 and 4 BKS in 2008. The BKS SR at 532nm was inferred from the 940 nm channel using a conversion factor of 0.254 ± 8%, an empirical factor derived from past measurements of stratospheric aerosol distributions.

[16] The sondes mean profiles are compared in Figure 5 with the mean CALIOP SR at 532 nm over Niamey during the 16 days encompassing the balloon flights and within ±7° latitude and ±70° longitude to account for aerosol transport assuming 1 m/s and 10 m/s for the meridional and zonal wind, respectively. After applying the cloud mask, the CALIOP profiles before (dotted black line) and after recalibration (solid black line) are shown in Figure 5. A SR increase at almost all levels, by 4% in August 2006 and 5% in September 2008, is seen after applying the adjustment. Below 17 km the BKS signal is affected by the presence of clouds. The amplitude of the Soufrière plume in 2006 at 18.5–22 km in both data sets is comparable. The altitude of the peak is slightly

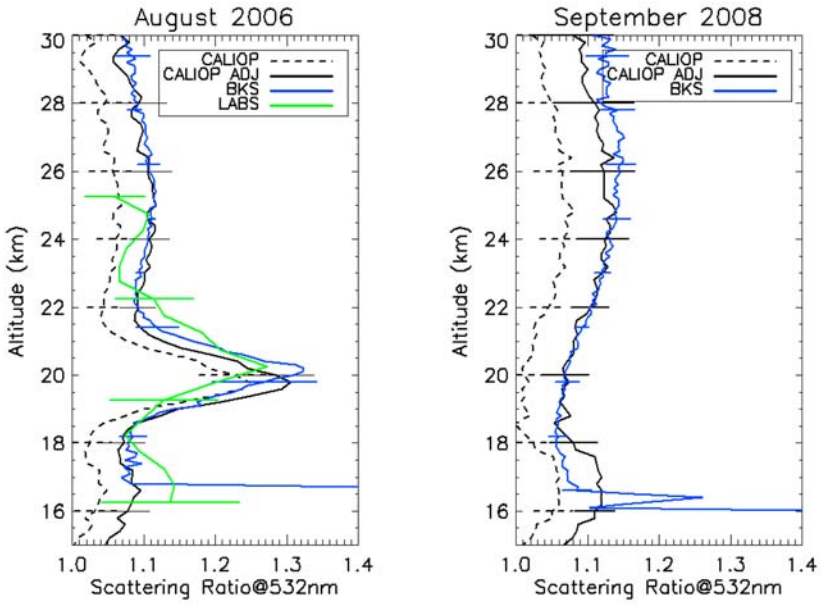

Figure 5. Mean CALIOP SR before (dotted black) and after recalibration and cloud mask application (CALIOP ADJ, solid black) within a ±7° latitude and ±70° longitude box centered in Niamey, mean BKS sonde SR at 940 nm normalized at 532 nm (blue), and LABS SR (green) for (left) August 2006 and (right) September 2008. The error bars show the respective standard deviations of the measurements.

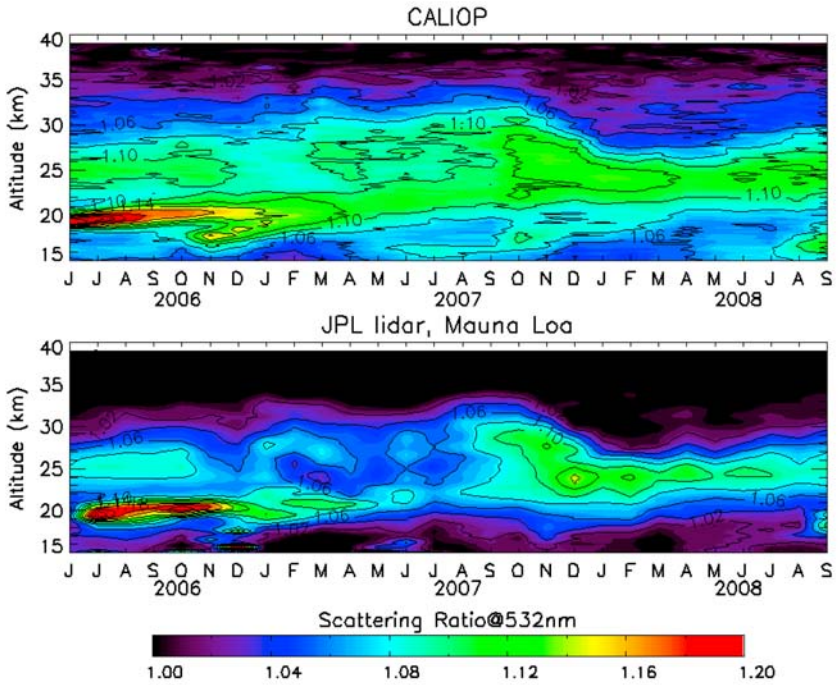

Figure 6. (top) Mean CALIOP SR within a ±7° latitude and ±70° longitude box centered in Hawaii (19.5°N–155.6°W) and (bottom) Mauna Loa Observatory JPL lidar scattering ratio at 532 nm converted from measurements at 355 nm.

different but this is not significant given the small number of BKS and LABS sondes flights during which the shape of the plume profile was varying from one flight to another. Note that because of the different nature of the particles, the conversion of the BKS data from 940 to 532 nm may not be as accurate as for background aerosols (J. Rosen, personal communication, 2008). In September 2008 the CALIOP SR in the northern part of its ±7° latitude band displays a volcanic plume below 18 km originating from an eruption in Alaska in July and later transported to the tropics (OMI, http://so2.umbc.edu/omi/omi_images.html). Above 22 km in August 2006 and 18 km in September 2008, the difference between CALIOP BKS and LABS is insignificant within their respective standard deviations (±1.5% BKS, ±5% LABS, ±% CALIOP at 24 km). In 2008, a difference appears above 25 km but still within the two sigma dispersion of the 4 BKS flights. Finally and importantly, the BKS measurements confirm the CALIOP observations of relatively clean air in the TTL between the cloud top and 18.5 km in 2006, and between 17 and 21 km in 2008.

3.4. Comparison With Ground-Based Lidar

[17] The corrected CALIOP SR profiles have been compared to the aerosol observations derived from the NASA-Jet Propulsion Laboratory (JPL) ozone lidar [*McDermid et al.*, 1995] located at the Mauna Loa Observatory in Hawaii (19.5°N, 155.6°W), part of the Network for Detection of Atmospheric Composition Change (NDACC). The JPL lidar data used here are the scattering ratios at 355 nm derived from the total backscatter at 355 nm and the nitrogen Raman channel at 387 nm used as a reference to compute the molecular backscatter. The signal is further corrected for molecular extinction and normalized at 34 ± 2 km by visual check. The SR profiles at 355 nm are converted to 532 nm using the wavelength exponent $Kb = -1.3$ characteristic of a stratospheric background aerosol level between 1997 and 1999 [*Jäger et al.*, 1995; *Jäger and Deshler*, 2002], following equations (3), (4), and (5):

$$\beta_{mie,\lambda 2} = \beta_{mie,\lambda 1} \times \left(\lambda_2 \Big/ \lambda_1\right)^{Kb} \tag{3}$$

$$\beta_{rayl} \propto \lambda^{-4.09} \tag{4}$$

$$(SR_{\lambda 2} - 1) = (SR_{\lambda 1} - 1)\left(\lambda_2 \Big/ \lambda_1\right)^{4.09+Kb} \tag{5}$$

where $\lambda_2 = 532$ nm and $\lambda_1 = 355$ nm.

[18] Figure 6 shows a comparison between the CALIOP mean SR within ±7° latitude and ±70° longitude after applying the cloud mask and the JPL lidar data during the same period. The pictures provided by the two systems are very similar displaying the same volcanic plumes including that of the Kasatochi eruption in August 2008 at about 16–17 km. They also show the same evolution of the aerosol in the midstratosphere including a minimum in the winter–spring 2007 between the vanishing old plume from the Mamam eruption, seen earlier by SAGE II, and the uplift of that from the Soufrière Hills. The two data sets show very high linear correlation above 20 km (r = 0.95). However, The JPL lidar profiles are systematically cut off at the bottom (near 17–19 km) when one or several thin Mie scattering layers are identified below 18 km. The resulting cloud or

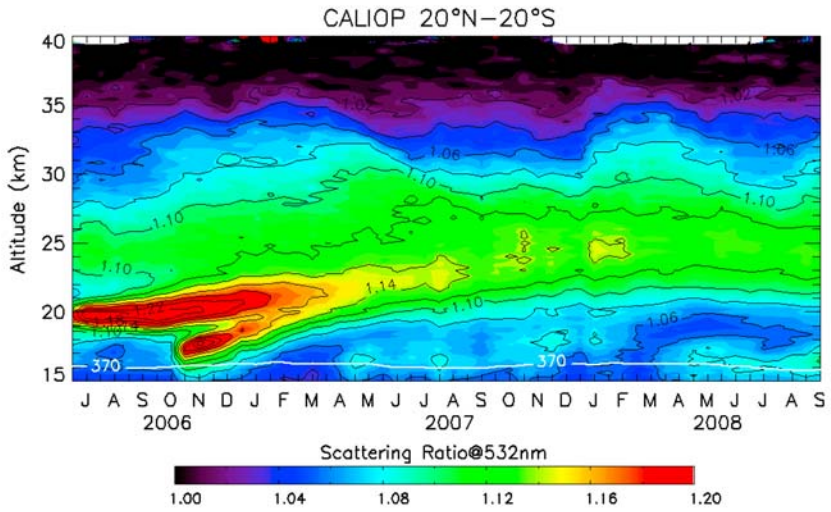

Figure 7. Same as Figure 1 after recalibration and cloud removal.

aerosol layer removal is likely responsible for the lower BSR values calculated for the JPL lidar below 18 km compared to CALIOP. In addition, small differences between the ground-based and space-borne lidars can also be explained by the uncertainty in the actual wavelength exponent backscatter used to convert the lidar profiles from 355 nm to 532 nm. Finally, and although the 2006–2008 period cannot be qualified as a background aerosol period, particularly in the lower stratosphere, the JPL lidar and CALIOP do show some maximum aerosol above 18 km during the winter, consistent with the 1996–2001 observations of *Barnes and Hofmann* [2001] of the NOAA-CMDL lidar at 532 nm also at Mauna Loa.

4. Revised Stratospheric Aerosols Picture in the Tropics

[19] The revised aerosol altitude-time cross section of the zonal 20°S–20°N average after applying the calibration adjustment and the cloud mask is shown in Figure 7. There are no more SR values lower than 1 ± 0.1 either at the top or at the bottom of the stratosphere. The average SR at 30–34 km is 1.06 with fluctuations of ±4% amplitude. There are fewer anomalies along the ascent of the Soufrière plume. Enhanced aerosol can be seen for example in January 2008 extending to all altitudes, suggesting an imperfect calibration adjustment. A possible explanation for that is the accuracy of the GEOS-5 temperature at high altitude. Indeed, an examination of the GEOS-5 temperature profiles shows a sudden decrease of 5°C at 36–39 km between 16 and 31 December 2007 and 1–16 January 2008, leading to a 3% change in the Rayleigh scattering. The sharp simultaneous aerosol increase by 3% at all levels between the two periods suggests that the temperature change in the GEOS-5 model could be underestimated.

[20] The Tavurvur plume at 17–19 km, previously partly masked by the clouds, is also shown in Figure 7. It ascended rapidly at an apparent vertical velocity of 0.6 km/month (0.2 mm/s) and was replaced within two months by clean air. Most remarkable is the lifting of clean air of SR < 1.02–1.04 above the tropopause, first to the maximum cloud top altitude around 18 km in December, then higher up to 19–20 km in February–March in both years and remaining at that altitude for several months. The stagnation of the cleansed air at this level is similar to that of the Soufrière plume from June to November 2006, indicating near-zero vertical velocity at least in the summer in this altitude range.

[21] Though of higher space and time resolution, the CALIOP SR picture is very consistent with that of the SAGE II v6.20 aerosol extinction ratio at 1020 nm between 1998 and 2005, after subtracting the molecular component using density from the NCEP meteorological model, shown in Figure 8. SAGE II shows the injection of two earlier volcanic plumes followed by their slow ascent in the mid-stratosphere: the first starting at 18.5 km in September 2002 attributed to Raventador at 0°N in Ecuador, and the second at 19.5 km in February 2005 to Manam in Papua New Guinea at 4°S. The plume from the latter is still present in the CALIOP measurements at 25 km in July 2006 at the beginning of the mission. Also confirmed by SAGE II is the spring–summer aerosol minimum above the cloud tops between 18 and 21 km.

[22] Further details on the altitude-latitude evolution of the CALIOP aerosols are provided by the series of latitudinal cross sections shown in Figure 9, corresponding to identical 16 day periods for the 3 years, selected for the maximum amplitude of events described below. The data displayed are calculated within 1° latitude zonal bands and thus have about 9% precision.

[23] At the beginning of the mission on 1–16 July 2006, both the Soufrière plume at 19–20.5 km between 8°S and 22°N, and the remnant around 25 km of that from Manam observed by SAGE II were visible. One and a half months later on 16–31 August, the Soufrière plume was slightly thicker with its top shifted upward by a few hundred meters but still in the same latitude range. The 16–31 October 2006 plot shows the Tarvurvur plume at 17 km between 15°S and 10°N roughly centered at the latitude of the eruption at 5°S. Two months later, on 16–31 December 2006, its plume was spread over a broad latitude range between 40°S and 30°N, while that of the Soufriere at 20 km was still confined within the tropics but with a higher top. At the lower levels between 5°S and 10°N, the Tavurvur plume was then replaced by

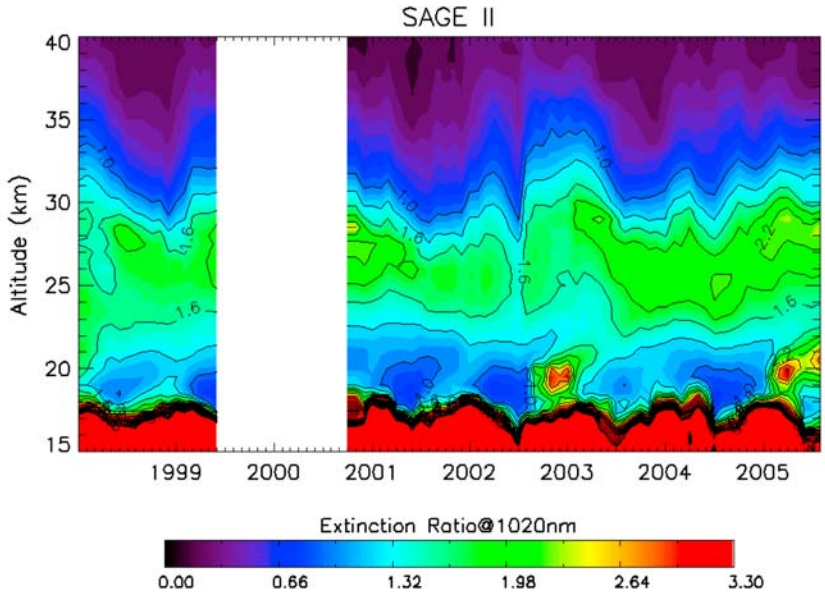

Figure 8. Altitude-time cross section of SAGE II zonal mean extinction ratio within 20°S–20°N from 1998 to the end of the mission in mid-2005.

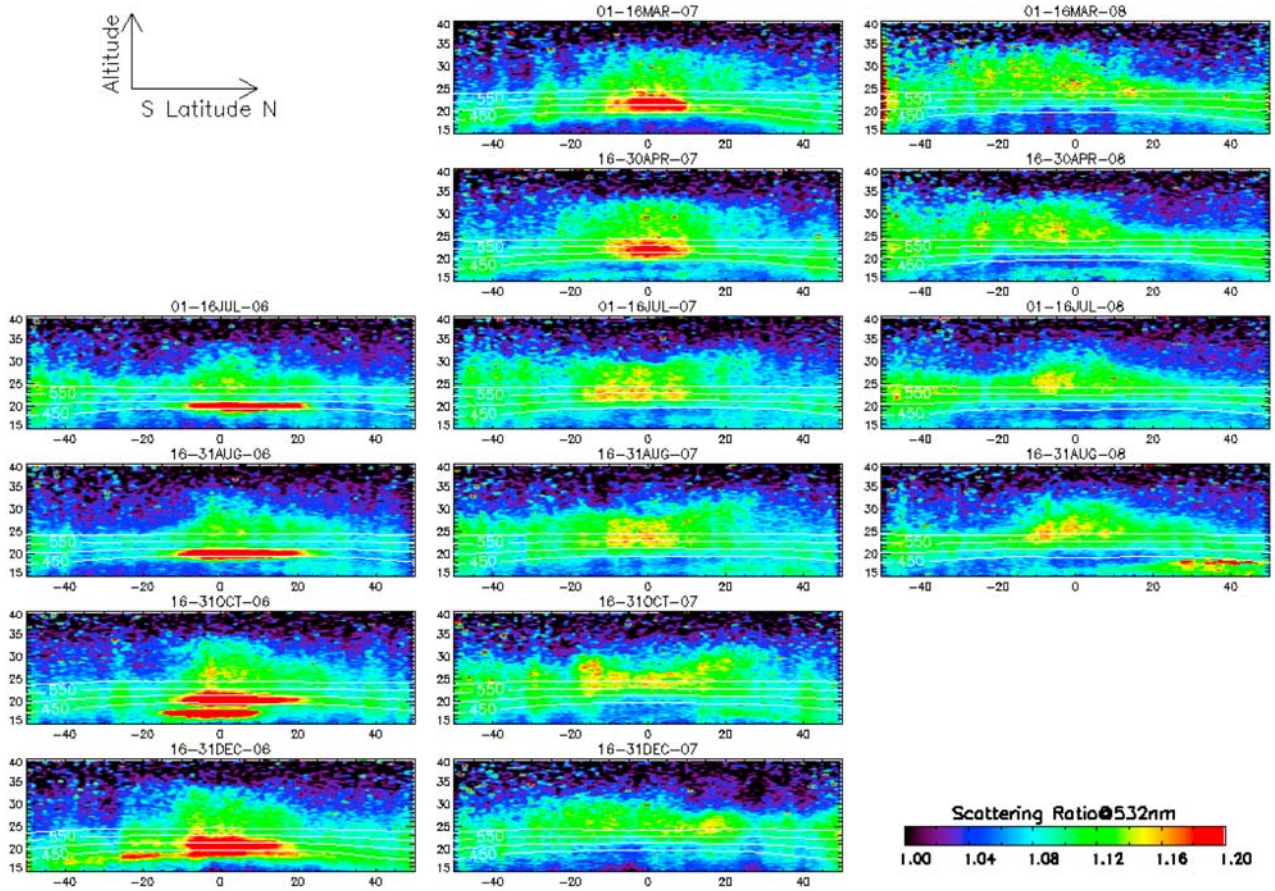

Figure 9. Altitude-latitude cross sections of CALIOP SR at selected periods since the beginning of the mission. Superimposed are the potential temperature levels at 370 K (tropopause), 450, 500, 550, and 600 K.

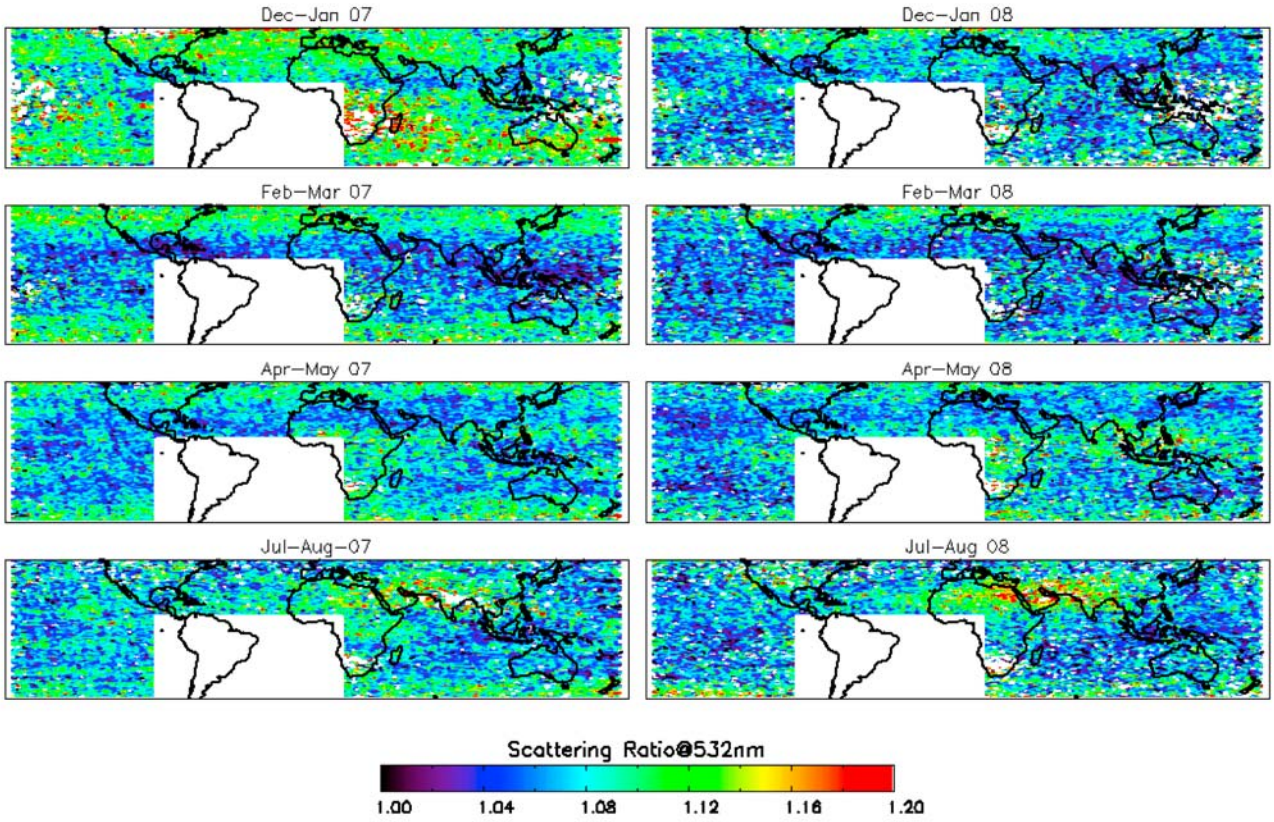

Figure 10. Geographical distribution of 2 month mean CALIOP SR between 16.5 and 17.5 km after applying the cloud mask (depolarization volume < 5%) and removing the noisy SAA signal (white rectangle) for December–January, February–March, April–May, and 1 July to 15 August (left) 2007 and (right) 2008.

cleaner air. Two and half months later on 1–16 March 2007, the top of the Soufriere plume continued to expand to higher altitude and a general cleansing of the TTL was observed between 35°S and 30°N. On 16–30 April 2007, the upper part of the Soufrière plume was still confined within 25°S–15°N but reached 30 km. At 16–17 km (Figure 1), weak depolarizing particles layer can be seen between 20°S and 10°N, also present in the following year at the same season. The 1–16 July 2007 plot exhibits a double horned vertical propagation of the Soufrière plume toward the subtropics at 30 km during the west phase of the QBO in contrast to the vertical uplift at the equator during the east phase in 2006 and 2008 as already noted by *Trepte and Hitchman* [1992] from SAGE II. Most remarkable in the following picture, during 16–31 August 2007, is the presence of another little depolarizing particles layer at 16–17 km but at northern latitudes between 15 and 40°N, also present in 2006 and 2008 during the same period. Next, during 16–31 October 2007, is a reinforced double horn B-D transport in the middle stratosphere and the addition of a new volcanic plume at most northern latitudes at 17–18 km after the eruption of Jebel-Al-Tair at 15.5 °N in Yemen on 30 September 2007 transported to midlatitude as shown by the SO_2 cloud reported by the AURA-OMI satellite (http://so2.umbc.edu/omi/omi_images.html). Most remarkable during 16–31 December 2007 is the restart of the cleansing of the TTL similar to that observed during the previous winter, reaching a maximum amplitude and altitude during 1–16 March. The 16–30 April 2008 picture shows a repetition of the 2007 little depolarizing particles episode at 16–17 km between 20°S and 10°N. The 1–16 July 2008 plot confirms the midstratosphere uplift in the equatorial belt during the easterly phase of the QBO similar to that of 2006 and again the presence of particles at 16–17 km over South Asia. Finally, the 16–31 August 2008 picture still shows the particles layer at 16–17 km around 10°–40°N but also the arrival from the north of a new plume injected by the Okmok and Kasatochi volcanoes in the Aleutian Islands on 12 July and 7 August 2008, further transported to lower latitudes at the end of August (AURA/OMI http://so2.umbc.edu/omi/omi_images.html).

[24] Figure 10 shows maps of 2 month mean SR between 16.5 and 17.5 km, which is near highest cloud tops, of particles with a volume depolarization ratio less than 5%. From top to bottom are December–January, February–March, April–May, and 1 July to 15August in 2007 and 2008, the last period being chosen for avoiding possible interference with Aleutian volcanic plumes at the end of August 2008. December–January 2006–2007 shows the volcanic aerosols of Tavurvur at 17 km, transported rapidly to northern and southern midlatitudes and reducing during the following months. This map also reveals missing data (white pixels) over Micronesia, due to the removal of clouds in the algorithm, known to be a zone where the occurrence of cirrus clouds is maximum [*Wang et al.*, 1996; *Sassen et al.*, 2008]. High

clouds can also be seen above Austral Africa and northern Australia, the most convective areas during this period. Similar cirrus (white pixels) are seen at the same season on the following year but shifted to the west above Indonesia. The difference with the previous winter is likely coming from the ENSO, shifting from a weak El Nino phase in winter 2006–2007 to La Nina in 2007–2008. February–March maps correspond to the period of cleansing of the TTL showing low SR (<1.04) everywhere between ±20° latitude. The maps in April–May, if compared to the previous, show areas of faint SR (1.08–1.12) and little depolarizing particles between 15°N and 20°S, which seems to be located over Africa, extending to SE Asia in 2008, during the most convective season in both cases. Finally, the bottom maps between July and mid-August show bands of little depolarizing particles with higher values of SR reaching 1.20 and extending from northern India, to south Arabia and North Africa, more intense in 2008.

[25] The nature of these particles is still unknown, and cannot be identified unambiguously from CALIOP observations alone. However, several remarks regarding their occurrence can be derived from Figure 10. The particles are not directly connected to high cirrus. Indeed, they are absent in December–January over the warm pool, the season and area of highest cirrus clouds. They seem to be observed over continents during most convective monsoon periods, thus in the absence of biomass burning, but next to desert areas and thus possibly related to mineral dust, although these are known to depolarize. The maximum over South Asia during the monsoon season could also be related to the transport of sulphur dioxide in convective systems near the cold point tropopause where oxidation by radical OH could lead to create new particles. More investigations are required to confirm these hypothesis.

[26] In summary, above 20 km, the picture provided by the first 2 years CALIOP measurements is very consistent with the known slow ascent in the tropics associated with the Brewer-Dobson circulation and the QBO modulation of the meridional transport toward the subtropics shown by *Trepte and Hitchman* [1992] from the SAGE II extinction and *Barnes and Hofmann* [2001] from the series of the NOAA ground-based lidar observations at Mauna Loa Observatory. However, newest information resides in the TTL. Indeed, aside from the known minimum vertical velocity around 20 km at the bottom of the BD circulation [*Hartmann et al.*, 2001; *Holton and Gettelman*, 2001; *Corti et al.*, 2005; *Fu et al.*, 2007; *Yang et al.*, 2008]. CALIOP observations are exhibiting two new features: (1) a seasonal apparent uplift of clean air from the tropopause up to the 500 K (20 km) peaking in February–March and (2) the presence of little depolarizing particles above cloud tops around 16.5–17.5 km, over land monsoon convective regions.

5. Conclusions and Implications for the Vertical Transport in the Lower Stratosphere

[27] A procedure for studying the evolution of the aerosols in the tropical stratosphere using CALIOP lidar data has been explored. After removing noisy data in the SAA region and applying appropriate averaging and cloud masking, it is shown that the current calibration of the operational products requires adjustment at low latitudes. Indeed, the presence of significant amounts of aerosols up to 35 km in the tropics, in contrast to midlatitudes, makes the current calibration procedure based on the assumption of pure Rayleigh scattering between 30 and 34 km inadequate at low latitudes. This leads to an average underestimation of the aerosol scattering ratio by 6%. A better picture is obtained by adjusting the calibration at higher level, 36–39 km, where SAGE II has reported an almost complete absence of aerosols in the past, although some artifacts are still present with 2–3% amplitude which could be related to errors in the temperature in the GEOS-5 at this altitude level.

[28] The revised picture of the evolution of the aerosols since the beginning of the CALIPSO mission in June 2006 until September 2008, is found to be very consistent with the information available from SAGE II prior to the end of its mission in 2005, with balloon in situ measurements in Africa in 2006 and 2008, as well as JPL lidar aerosol profiles in Hawaii. After applying these corrections, the CALIOP lidar is shown to provide the highest ever time and space resolution information on the three-dimensional transport from the tropopause to 40 km.

[29] In the stratosphere, the observed average ascent rate of the volcanic aerosols at 200 m/month (0.08 mm/s) at 22 km (40 hPa) is consistent with recent heating rate calculations [*Yang et al.*, 2008], though a little slower, as well as with the near-zero vertical velocity around 20 km at the bottom of the tropical pipe [*Plumb*, 1996]. The influence of the QBO on the Brewer-Dobson circulation in the midstratosphere showing faster meridional transport toward the subtropics during the westerly phase is also confirmed.

[30] New findings in the CALIOP observations below 20 km are the seasonal uplift of clean air from the tropopause up to the minimum velocity level around 19–20 km in February–March, and the presence of little depolarizing particles or aerosols of unknown nature immediately above cloud tops at 16.5–17.5 km over continents during monsoon periods nearby deserts area. The fast uplift of clean air masses up to around 19 km within less than one month in February–March is comparable to that of CO reported by the AURA-MLS during the same season in 2005, which was shown to have occurred primarily over equatorial Africa and to a lesser extent over Indonesia [*Schoeberl et al.*, 2006]. The transport of this clean air seems to occur within one month or less with a vertical velocity 3–4 times faster than the maximum average speed in the winter derived from radiative heating calculations [*Yang et al.*, 2008] and might imply an underestimation of the velocity in those calculations or an additional mechanism. The coincidence of these events with the beginning of the season and region of maximum overshooting volume reported by the TRMM precipitation radar [*Liu and Zipser*, 2005] would suggest that convective overshooting might also contribute at least up to 19 km. Note that CO [*Schoeberl et al.*, 2006] and N_2O [*Ricaud et al.*, 2009] show another seasonal maximum in September–November over Amazonia in CO but of lesser altitude extent. Unfortunately, nothing can be said about clean air there since CALIOP observations are not available over this region because of the presence of the SAA. Finally, the stagnation or the very slow ascent of clean air for several months at around 19 km is consistent with the observed CO seasonal maximum at 68 hPa (18.5 km) shifted by about 1–2 months compared to 100 hPa after taking into account the chemical lifetime of the species

[*Randel et al.*, 2007] or the N_2O maximum in November–January at the same altitude [*Ricaud et al.*, 2009]. However, the limited 4 km vertical resolution of the MLS and SMR in a region of steep vertical gradient of the species does not allow precise information on the altitude dependence of the vertical velocity to be derived, in contrast to the high-resolution CALIOP measurements which seems to indicate a fast detrainment of clean air up to 19 km in February–March.

[31] It is hoped that further improvements to the CALIOP calibration and the continuation of the mission, as well as microphysical particle and cloud modeling, will help clarifying the relative contributions of radiative heating and convective overshoot to the vertical transport from the tropopause to the base of the tropical pipe.

[32] **Acknowledgments.** The CALIOP data are processed at NASA LaRC and made available at the ICARE data center (http://www-icare.univ-lille1.fr/). The SAGE II data are those available at http://eosweb.larc.nasa.gov/. The JPL ozone lidar data from Mauna Loa, Hawaii, are made publicly available at the NDACC Data Handling Facility (http://www.ndsc.ncep.noaa.gov/). The authors thank the AMMA organization team in Niger and the CNES French Space Center for their help in the balloon-sonde flights. The authors are thankful to Jim Rosen and Terry Deshler for sharing their expertise on the backscatter sondes and the optical particles counters. The project was supported by CNES-CALIPSO and the LEFE CNRS Tropical UTLS project in France and the EU SCOUT-O3 project (505390-GOCE-CT-2004).

References

Adriani, A., F. Cairo, S. Mandolini, G. Di Donfrancesco, T. Deshler, and B. Nardi (1996), A new joint balloon-borne experiment to study polar stratospheric clouds: Laser backscatter sonde and optical particle counter, in *Atmospheric Ozone: Proceedings of the 18th Quadriennal Ozone Symposium 1996 and Tropospheric Ozone Workshop*, edited by R. D. Bojkov and G. Visconti, pp. 879–882, Parco Sci. e Tecnol. d'Abruzzo, L'Aquila, Italy.

Barnes, J. E., and D. J. Hofmann (2001), Variability in the stratospheric background aerosol over Mauna Loa Observatory, *Geophys. Res. Lett.*, *28*, 2895–2898, doi:10.1029/2001GL013127.

Brewer, A. W. (1949), Evidence for a world circulation provided by the measurements of helium and water vapor distribution in the stratosphere, *Q. J. R. Meteorol. Soc.*, *75*, 351–363, doi:10.1002/qj.49707532603.

Cairo, F., G. Di Donfrancesco, A. Adriani, L. Pulvirenti, and F. Fierli (1999), Comparison of various linear depolarization parameters measured by lidar, *Appl. Opt.*, *38*, 4425–4432, doi:10.1364/AO.38.004425.

Cairo, F., et al. (2009), An overview of the SCOUT-AMMA stratospheric aircraft, balloons and sondes campaign in West Africa, August 2006: Rationale, roadmap and highlights, *Atmos. Chem. Phys. Discuss.*, *9*, 19,713–19,781.

Carn, S. A., N. A. Krotkov, K. Yang, R. M. Hoff, A. J. Prata, A. J. Krueger, S. C. Loughlin, and P. F. Levelt (2007), Extended observations of volcanic SO_2 and sulfate aerosol in the stratosphere, *Atmos. Chem. Phys. Discuss.*, *7*, 2857–2871.

Chu, W. P., M. P. McCormick, J. Lenoble, C. Brogniez, and P. Pruvost (1989), SAGE II inversion algorithm, *J. Geophys. Res.*, *94*, 8339–8351, doi:10.1029/JD094iD06p08339.

Corti, T., B. P. Luo, P. Peter, H. Vömel, and Q. Fu (2005), Mean radiative energy balance and vertical mass fluxes in the equatorial upper troposphere and lower stratosphere, *Geophys. Res. Lett.*, *32*, L06802, doi:10.1029/2004GL021889.

Danielsen, E. F. (1982), A dehydration mechanism for the stratosphere, *Geophys. Res. Lett.*, *9*, 605–608, doi:10.1029/GL009i006p00605.

Danielsen, E. F. (1993), In situ evidence of rapid, vertical, irreversible transport of lower tropospheric air into the lower stratosphere by convective cloud turrets and by larger scale upwelling in tropical cyclones, *J. Geophys. Res.*, *98*, 8665–8681, doi:10.1029/92JD02954.

Fu, Q., Y. Hu, and Q. Yang (2007), Identifying the top of the tropical tropopause layer from vertical mass flux analysis and CALIPSO lidar cloud observations, *Geophys. Res. Lett.*, *34*, L14813, doi:10.1029/2007GL030099.

Fueglistaler, S., A. E. Dessler, T. J. Dunkerton, I. Folkins, Q. Fu, and P. W. Mote (2009), Tropical tropopause layer, *Rev. Geophys.*, *47*, RG1004, doi:10.1029/2008RG000267.

Hartmann, D. L., J. R. Holton, and Q. Fu (2001), The heat balance of the tropical tropopause, *Q. J. R. Meteorol. Soc.*, *124*, 1579–1604.

Hitchman, M. H., M. McKay, and C. R. Trepte (1994), A climatology of stratospheric aerosol, *J. Geophys. Res.*, *99*, 20,689–20,700, doi:10.1029/94JD01525.

Holton, J. R., and A. Gettelman (2001), Horizontal transport and the dehydration of the stratosphere, *Geophys. Res. Lett.*, *28*, 2799–2802, doi:10.1029/2001GL013148.

Holton, J. R., P. H. Haynes, M. E. McIntyre, A. R. Douglass, R. B. Rood, and L. Pfister (1995), Stratosphere-troposphere exchange, *Rev. Geophys.*, *33*, 403–439, doi:10.1029/95RG02097.

Hostetler, C. A., Z. Liu, J. Regan, M. Vaughan, D. Winker, M. Osborn, W. H. Hunt, K. A. Powell, and C. Trepte (2006), CALIOP Algorithm Theoretical Basis Document (ATBD): Calibration and level 1 data products, *Doc. PC-SCI-201*, NASA Langley Res. Cent., Hampton, Va. (Available at www-calipso.larc.nasa.gov/resources/pdfs/PC-SCI-201v1.0.pdf)

Jäger, H., and T. Deshler (2002), Lidar backscatter to extinction, mass and area conversions for stratospheric aerosols based on mid-latitude balloon-borne size distribution measurements, *Geophys. Res. Lett.*, *29*(19), 1929, doi:10.1029/2002GL015609.

Jäger, H., T. Deshler, and D. J. Hofmann (1995), Mid-latitude lidar backscatter conversions based on balloon-borne aerosol measurements, *Geophys. Res. Lett.*, *22*, 1727–1732.

Khaykin, S., et al. (2009), Hydration of the lower stratosphere by ice crystal geysers over land convective systems, *Atmos. Chem. Phys.*, *9*, 2275–2287.

Liu, C. (2007), Geographical and seasonal distribution of tropical tropopause thin clouds and their relation to deep convection and water vapor viewed from satellite measurements, *J. Geophys. Res.*, *112*, D09205, doi:10.1029/2006JD007479.

Liu, C., and E. J. Zipser (2005), Global distribution of convection penetrating the tropical tropopause, *J. Geophys. Res.*, *110*, D23104, doi:10.1029/2005JD006063.

Liu, C., and E. J. Zipser (2009), Implications of the day versus night differences of water vapor, carbon monoxide, and thin cloud observations near the tropical tropopause, *J. Geophys. Res.*, *114*, D09303, doi:10.1029/2008JD011524.

Liu, C., E. Zipser, T. Garrett, J. H. Jiang, and H. Su (2007), How do the water vapor and carbon monoxide "tape recorders" start near the tropical tropopause?, *Geophys. Res. Lett.*, *34*, L09804, doi:10.1029/2006GL029234.

McCormick, M., and R. Veiga (1992), SAGE II measurements of early Pinatubo aerosols, *Geophys. Res. Lett.*, *19*, 155–158, doi:10.1029/91GL02790.

McCormick, M. P., L. W. Thomason, and C. R. Trepte (1995), Atmospheric effects of the Mt. Pinatubo eruption, *Nature*, *373*, 399–404, doi:10.1038/373399a0.

McDermid, I. S., T. D. Walsh, A. Deslis, and M. L. White (1995), Optical systems design for a stratospheric lidar, *Appl. Opt.*, *34*, 6201–6210, doi:10.1364/AO.34.006201.

Mote, P. W., K. H. Rosenlof, M. E. McIntyre, E. S. Carr, J. C. Gille, J. R. Holton, J. S. Kinnersley, H. C. Pumphrey, J. M. Russell, and J. W. Waters (1996), An atmospheric tape recorder: The imprint of tropical tropopause temperatures on stratospheric water vapor, *J. Geophys. Res.*, *101*, 3989–4006, doi:10.1029/95JD03422.

Nazaryan, H., M. P. McCormick, and W. P. Menzel (2008), Global characterization of cirrus clouds using CALIPSO data, *J. Geophys. Res.*, *113*, D16211, doi:10.1029/2007JD009481.

Osborn, M. T., G. S. Kent, and C. R. Trepte (1998), Stratospheric aerosol measurements by the Lidar in Space Technology Experiment, *J. Geophys. Res.*, *103*, 11,447–11,453, doi:10.1029/97JD03429.

Plumb, R. A. (1996), A 'tropical pipe' model of stratospheric transport, *J. Geophys. Res.*, *101*, 3957–3972, doi:10.1029/95JD03002.

Pommereau, J.-P., and G. Held (2007), Is there a stratospheric fountain?, *Atmos. Chem. Phys. Discuss.*, *7*, 8933–8950.

Prata, A. J., S. A. Carn, A. Stohl, and J. Kerkmann (2007), Long range transport and fate of a stratospheric volcanic cloud from Soufrière Hills volcano Montserrat, *Atmos. Chem. Phys.*, *7*, 5093–5103.

Randel, W. J., M. Park, F. Wu, and N. Livesey (2007), A large annual cycle in ozone above the tropical tropopause linked to the Brewer-Dobson circulation, *J. Atmos. Sci.*, *64*, 4479–4488, doi:10.1175/2007JAS2409.

Ricaud, P., B. Barret, J.-L. Attié, E. Le Flochmoën, E. Motte, H. Teyssèdre, V.-H. Peuch, N. Livesey, A. Lambert, and J.-P. Pommereau (2007), Impact of land convection on troposphere-stratosphere exchange in the tropics, *Atmos. Chem. Phys.*, *7*, 5639–5657.

Ricaud, P., J.-P. Pommereau, J.-L. Attié, E. Le Flochmoën, L. El Amraoui, H. Teyssèdre, V.-H. Peuch, W. Feng, and M. P. Chipperfield (2009), Equatorial transport as diagnosed from nitrous oxide variability, *Atmos. Chem. Phys.*, *9*, 8173–8188.

Rosen, J. M., and N. T. Kjome (1991), The backscattersonde: A new instrument for atmospheric aerosol research, *Appl. Opt.*, *30*, 1552–1561, doi:10.1364/AO.30.001552.

Sassen, K., Z. Wang, and D. Liu (2008), Global distribution of cirrus clouds from CloudSat/Cloud-Aerosol Lidar and Infrared Pathfinder Satellite Observations (CALIPSO) measurements, *J. Geophys. Res.*, *113*, D00A12, doi:10.1029/2008JD009972.

Schoeberl, M. R., B. N. Duncan, A. R. Douglass, J. Waters, N. Livesey, W. Read, and M. Filipiak (2006), The carbon monoxide tape recorder, *Geophys. Res. Lett.*, *33*, L12811, doi:10.1029/2006GL026178.

Sherwood, S. C., and A. E. Dessler (2000), On the control of stratospheric humidity, *Geophys. Res. Lett.*, *27*, 2513–2516, doi:10.1029/2000GL011438.

Thomason, L. W., and T. Peter (Eds.) (2006), Assessment of Stratospheric Aerosol Properties (ASAP), *SPARC Rep. 4*, World Clim. Res. Programme, Geneva, Switzerland.

Thomason, L. W., M. C. Pitts, and D. M. Winker (2007), CALIPSO observations of stratospheric aerosols: A preliminary assessment, *Atmos. Chem. Phys.*, *7*, 5283–5290.

Trepte, C. R., and M. H. Hitchman (1992), Tropical stratospheric circulation deduced from satellite aerosol data, *Nature*, *355*, 626–628, doi:10.1038/355626a0.

Vaughan, M., S. Young, D. Winker, K. Powell, A. Omar, Z. Liu, Y. Hu, and C. Hostetler (2004), Fully automated analysis of space based lidar data: An overview of the CALIPSO retrieval algorithms and data products, *Proc. SPIE Int. Soc. Opt. Eng.*, *5575*, 16–30, doi:10.1117/12.572024.

Wang, P.-H., P. Minnis, M. P. McCormick, G. S. Kent, and K. M. Skeens (1996), A 6-year climatology of cloud occurrence frequency from Stratospheric Aerosol and Gas Experiment II observation (1985–1990), *J. Geophys. Res.*, *101*, 29,407–29,429, doi:10.1029/96JD01780.

Winker, D. M., J. Pelon, and M. P. McCormick (2003), The CALIPSO mission: Space borne lidar for observation of aerosols and clouds, *Proc. SPIE Int. Soc. Opt. Eng.*, *4893*, 1–11, doi:10.1117/12.466539.

Winker, D. M., W. H. Hunt, and M. J. McGill (2007), Initial performance assessment of CALIOP, *Geophys. Res. Lett.*, *34*, L19803, doi:10.1029/2007GL030135.

Yang, Q., Q. Fu, J. Austin, A. Gettelman, F. Li, and H. Vömel (2008), Observationally derived and general circulation model simulated tropical stratospheric upward mass fluxes, *J. Geophys. Res.*, *113*, D00B07, doi:10.1029/2008JD009945.

F. Cairo, ISAC-CNR, Via Fosso del Cavaliere 100, I-00133 Rome, Italy.

T. Christensen, N. Larsen, and J. Nielsen, Danish Meteorological Institute, Lyngbyvej 100, DK-2100 Copenhagen, Denmark.

A. Garnier, J. Pelon, J. P. Pommereau, and J. P. Vernier, LATMOS, Université de Versailles Saint Quentin, CNRS, F-91371 Verrières le Buisson, France. (jean-paul.vernier@latmos.ipsl.fr)

T. Leblanc and I. S. McDermid, Jet Propulsion Laboratory, California Institute of Technology, Wrightwood, CA 92397, USA.

L. W. Thomason, NASA Langley Research Center, Mail Stop 475, Hampton, VA 23666, USA.